



Mapping Opium Poppy Cultivation: Socioeconomic Insights from Satellite Imagery

AROGYA KOIRALA, University of California, Berkeley, USA

SURAJ R NAIR, University of California, Berkeley, USA

XIAO HUI TAI, University of California, Davis, USA

Over 30 million people globally consume illicit opiates. In recent decades, Afghanistan has accounted for 70–90% of the world’s illicit supply of opium. This production provides livelihoods to millions of Afghans, while also funneling hundreds of millions of dollars to insurgent groups every year, exacerbating corruption and insecurity, and impeding development. Remote sensing and field surveys are currently used in official estimates of total poppy cultivation area. These aggregate estimates are not suited to study the local socioeconomic conditions surrounding cultivation. Few avenues exist to generate comprehensive, fine-grained data under poor security conditions, without the use of costly surveys or data collection efforts. Here, we develop and test a new unsupervised approach to mapping cultivation using only freely available satellite imagery. For districts accounting for over 90% of total cultivation, our aggregate estimates track official statistics closely (correlation coefficient of 0.76 to 0.81). We combine these predictions with other grid-level data sources, finding that areas with poppy cultivation have poorer outcomes such as infant mortality and education, compared to areas with exclusively other agriculture. Surprisingly, poppy-growing areas have better healthcare accessibility. We discuss these findings, the limitations of mapping opium poppy cultivation, and associated ethical concerns.

CCS Concepts: • Applied computing → Law, social and behavioral sciences;

Additional Key Words and Phrases: Illicit cultivation, satellite imagery, clustering

ACM Reference Format:

Arogya Koirala, Suraj R Nair, and Xiao Hui Tai. 2024. Mapping Opium Poppy Cultivation: Socioeconomic Insights from Satellite Imagery. *ACM J. Comput. Sustain. Soc.* 2, 2, Article 19 (May 2024), 29 pages. <https://doi.org/10.1145/3648435>

1 INTRODUCTION

Globally, over 30 million people consume illicit opiates (2021 estimates [58]). Only a few countries make up the bulk of the supply of this illicit opium, with Afghanistan being the world’s largest

A. Koirala and S. R Nair contributed equally to this research.

We are grateful to Tej Sathe for excellent research assistance, and to the anonymous reviewers for their thoughtful feedback. We thank Google and Google Earth Engine for hosting large geospatial data sets and making planetary-scale computational capabilities available to researchers. We also thank participants of COMPASS ’21 and at the Workshop on Humanitarian Mapping at KDD ’21 for feedback on early versions of this work. The authors did not receive specific funding for this work and declare no competing interests.

Authors’ address: A. Koirala and S. R. Nair, University of California, Berkeley, CA 94720, California, USA; e-mails: arogy@berkeley.edu, suraj.nair@ischool.berkeley.edu; X. H. Tai, University of California, Davis, CA 95616, California, USA; e-mail: xtai@ucdavis.edu.



This work is licensed under a Creative Commons Attribution-NonCommercial-ShareAlike International 4.0 License.

© 2024 Copyright held by the owner/author(s).

ACM 2834-5533/2024/05-ART19

<https://doi.org/10.1145/3648435>

supplier since 1999, accounting for an estimated 70–90% of supply [49, 58]. Apart from exerting a large influence on global drug markets, the cultivation of opium poppy has had significant implications on Afghanistan’s economic development, security situation, and rural communities. In 2019, opium cultivation generated an estimated income of \$1.2–\$2.1 billion domestically, or around 10% of Afghanistan’s gross domestic product [55]. Villages that cultivated opium poppy have been found (in surveys) to have poorer access to infrastructure and basic services, and experience more violence [55]. Yet few avenues exist to generate more comprehensive data and evidence on opium poppy cultivation and its associated local socioeconomic conditions, without the use of costly surveys or data collection efforts.

Over the years, efforts to monitor opium poppy cultivation in Afghanistan have been led by the United Nations Office of Drugs and Crime (UNODC). The UNODC releases annual reports containing aggregated estimates of opium cultivation, both at a province and at a district level (Afghanistan is divided into 32 provinces and 398 districts; district-level UNODC estimates are described as being “indicative”) [7, 49, 55]. The methodology involves field surveys and manual annotation of high-resolution (e.g., <1 m) satellite imagery. This approach produces valuable information, but is expensive and time-consuming, and difficult to undertake under poor security conditions. The Afghanistan government had previously been accused of blocking publication of poppy cultivation-related statistics [9]; in some years, reports are released with long delays.¹ In the past, the UNODC has additionally conducted separate surveys among village headmen in certain years to gather village-level information about poppy cultivation and socioeconomic conditions [55]. Given the current political environment, the future availability or reliability of official estimates or surveys is unclear.²

The focus of this work is to produce high-resolution maps of opium poppy cultivation, covering a large geographical area, using only freely available satellite imagery. Apart from cost and availability, there are numerous arguments for the production and use of such high-resolution maps, relative to aggregate statistics. A primary one is that many phenomena are local, and analyses conducted at an aggregated level obscure local patterns. With the public availability of high-resolution satellite imagery and other sources of granular data, there has been a proliferation of related research producing grid-level maps in numerous domains, for example, for economic development and public health-related outcomes (e.g., population [52], poverty [26], electrification [17], infant, and child mortality [14]). The availability of high-resolution cultivation maps will allow us to exploit these rich new sources of data to gain additional insight on local circumstances surrounding cultivation. Specific to the Afghan context, maps can overcome past over-reliance on aggregated cultivation statistics—previous counter-narcotics efforts have focused heavily on reducing overall opium cultivation area, which has been criticized as being counterproductive, because they do not take into consideration local socioeconomic challenges and the availability of alternative livelihoods [49]. Given the challenging political and security situation after the Taliban takeover, generating maps from freely-available data could be a valuable additional source of information on local conditions moving forward.

Mapping opium poppy relates more broadly to the rich literature on land cover classification as well as crop type mapping. However, existing methods do not transfer easily, since only major crops like wheat, maize, rice, and soybean are typically considered. While there has been some existing work using automated methods to detect the opium poppy crop using remotely sensed

¹For example, the report on the 2019 harvest season was only released in February 2021.

²Since the Taliban takeover in August 2021, a full report of 2021 cultivation statistics was released; as of May 2023, province-level cultivation statistics for the 2022 season have been released. No findings from socioeconomic surveys have been released to our knowledge.

data, these have been limited to experimental settings or specific study areas (e.g., in China, Laos, and Afghanistan). In many cases, researchers are able to either acquire high-resolution imagery (e.g., from unmanned aerial vehicles), proprietary ground truth data, or both, for their specific purposes [16, 28, 31, 32, 45, 60, 61, 67]. We are not aware of any other work that uses only publicly available data, on a large scale or over multiple years, to map opium poppy, which is the focus of our work.

In this article, we develop an automated approach to mapping opium poppy cultivation, using multi-spectral, high-resolution (up to 10 meters) satellite imagery. Drawing from the literature on crop type mapping and detection of opium poppy cultivation, we incorporate knowledge of growing seasons and crop types, and utilize unsupervised machine learning techniques. Specifically, we use vegetation indices to estimate optimal image acquisition dates to capture the opium poppy crop at pre-harvest and post-harvest dates; these two periods have been shown in other work to provide maximum discrimination between opium poppy and other crops. In these growth stages, the main other crop present is wheat, and we use the k -means algorithm to distinguish between these crops. We evaluate the accuracy of generated maps by comparing our estimates to aggregate district-level UNODC statistics from multiple years, with a particular focus on the top quartile of poppy-growing regions, accounting for over 90% of total cultivation. We achieve correlation coefficients of 0.76 to 0.81 with these indicative, “ground truth” data. Visual examination of clustering results is consistent with known crop characteristics.

Next, we demonstrate how the high-resolution maps that we produce can be combined with other data sources to further our understanding of the socioeconomic circumstances associated with poppy cultivation. This fine-grained analysis reveals notable differences between poppy-growing regions and other non-poppy agricultural areas. We find that agricultural areas with opium poppy have higher infant mortality and lower years of schooling. Surprisingly, they have better healthcare accessibility. Relative household wealth is slightly lower, and the Human Development Index (HDI), which incorporates information about income, education, and health, is also slightly lower. We discuss these findings and conclude by discussing ethical concerns, as well as the limitations of our approach. We make all our code and maps available at <https://github.com/arogyakoirala/poppy>.

2 RELATED WORK

Our work builds on literature in three areas: remote sensing-based land cover classification and crop type mapping, automatic approaches to detecting opium poppy, and the socioeconomic circumstances surrounding poppy cultivation.

2.1 Land Cover, Land Use Classification, and Crop Type Mapping

There is a vast literature on land cover and land use classification [12, 40, 50]. Typical land use classes are urban, agriculture, rangeland, forest, water bodies, and barren land [2]. Spectral properties (e.g., green, red, NIR, and SWIR bands and associated vegetation indices) are used to separate classes, broadly using either pixel-based or object-based methods. Pixel-based methods classify each pixel independently and are generally less computationally intensive, while object-based methods identify contiguous regions and then classify the regions [5]. From the literature on land use and land cover classification, we use existing maps of agricultural land to limit the area of our analysis. Our specific methodologies are more closely related to crop type mapping and in particular the identification of single crops. Existing work is described in this section, and details on how we adapted and extended existing methods to our work is in Section 3.

Crop type mapping typically focus on more commonly grown crops such as wheat, maize, rice and soybean, and the goal is typically to map multiple crops simultaneously. Temporal profiles are

often generated from imagery acquired at multiple time points throughout the year [18, 24]. Vegetation indices (such as the normalized difference vegetation index (NDVI)) are calculated at each time point, capturing information about crop cycles which can be used to differentiate between crops. Apart from using spectral properties at multiple time points directly, Fourier transforms have been used to derive features from time series profiles of both surface reflectance and vegetation indices [37, 62]. For classification, both unsupervised and supervised [e.g., 42] methods have been employed, for example, k -means, Gaussian mixture models (GMM) [e.g., 62], random forests, and deep learning approaches [e.g., 27]. For the identification of single crops, acquisition windows (for acquiring satellite imagery) may be timed for the optimal detection of that particular crop, either from knowledge of crop calendars or measured from the imagery (using indices such as the NDVI) [53]. For example, suitable acquisition timing may be a pre-harvest or post-harvest period, or multiple months corresponding to the phenological stages of the crop [8]. Such a strategy avoids using imagery from time periods which do not provide useful information about the particular crop. Spectral properties or vegetation indices are then used in a similar manner to generate features for unsupervised or supervised methods.

2.2 Automatically Detecting Opium Poppy

More specific to our problem, researchers have tested methods to specifically detect the opium poppy crop at a field-level. This has been done using satellite imagery as well as imagery from unmanned aerial vehicles and field spectrometers [16, 28, 31, 32, 45, 60, 61, 67]. A comprehensive review on detecting cannabis and opium crops is in [8]. Due to the illegal nature of the opium poppy crop, existing work has primarily been done under experimental settings [e.g., 28], or in collaboration with drug monitoring agencies that have access to ground truth data in a limited geographical area of interest [e.g., 60, 61]. Many of these studies are in Afghanistan, since majority of the world's opium cultivation occurs in the country. The processing and classification steps largely mirror those for crop type mapping for single crops; typical pre-processing of imagery includes atmospheric correction and the removal of cloudy pixels.

In terms of image acquisition, satellite imagery is first acquired during the appropriate period in the crop cycle, in particular pre-harvest, close to the peak in vegetation activity and when crops are flowering [28, 47, 53]. This is either done in experimental settings or guided by knowledge of crop calendars in poppy-growing areas. For supervised approaches, labels are obtained either through experimental settings, visual interpretation of known cultivation areas, or in collaboration with the UNODC. Specific methods that have been tested include classification and regression trees [28], maximum-likelihood [16], nearest neighbors [46], as well as deep learning approaches for object detection [31, 67], and semantic segmentation [32]. For unsupervised approaches, methods like Iterative Self-Organizing Data Analysis Technique (ISODATA), a variant of the standard k -means algorithm, have been used, as well as more specialized algorithms such as Multiple Endmember Spectral Mixture Analysis (MEMSA) [45, 60, 61]. Our analysis focuses on unsupervised methods, since these do not require manual annotation or access to previously constructed ground truth data sets. Ground truth data require expert knowledge and/or verification using ground images, which are not widely accessible or feasible.

While not an automated strategy, it is worth briefly reviewing the methodology for the production of official statistics released by the UNODC and the U.S. government in Afghanistan [7, 49, 55], since these are (to our knowledge) the only source of data covering a large geographical area, although at an aggregated level. In high-cultivation districts, high-resolution (e.g., <1 m) satellite imagery is acquired for sampled locations at a pre-harvest and post-harvest date. These are manually annotated; annotations from these sampled locations are then used to produce aggregated estimates, incorporating information about the sampling strategy. The sampling strategy is

Table 1. Distinguishing Characteristics of Wheat Versus Poppy

Crop	Harvest dates	Crop characteristics	
Poppy	April–June [53, 54]	Pre-harvest	NDVI: slowly increasing to a peak of around 0.6 [54] Appearance: Bright green [7, 31]
		Post-harvest	Fields often plowed immediately after harvest [54] Appearance: Light brown / beige [7]
Wheat	Typically right after poppy [22]	Pre-harvest	NDVI: consistently hovering around 0.8 [54] Appearance: Dark green [31]
		Post-harvest	Not plowed as quickly [54] Appearance: Dark brown

In many districts, particularly those with larger amounts of cultivation, these are the two main crops with similar growing seasons (barley is also cultivated, to a much smaller extent) [53]. Acquiring images at two dates, pre-harvest and post-harvest, allow for maximum discrimination between opium poppy and other crops [55].

designed to produce estimates at a province level, and while district-level estimates are released, they are described in the following way: “They are indicative and suggest a possible distribution of the estimated provincial poppy area among the districts of a province” [57].

2.3 Socioeconomic Circumstances Surrounding Poppy Cultivation

Another body of related work tries to understand risk factors and consequences of poppy cultivation. In general, while opium poppy is seen to be a lucrative cash crop, the literature points to negative spillovers, such as food insecurity, corruption and violence, drug addiction, and poorer development-related outcomes such as access to electricity grids, healthcare facilities, and schools for girls [55]. One source of such evidence is UNODC surveys of village headmen. The Afghanistan Research and Evaluation Unit has also studied local conditions and specific phenomena surrounding poppy cultivation, using qualitative and survey-based methods, as well as high-resolution satellite imagery [e.g., 33–35]. Other work has used official poppy cultivation estimates (released by UNODC) at a district or province-level to estimate the causal relationship between poppy cultivation and terrorism, infrastructure, and conflict [30, 41, 65]. In terms of risk factors, [29] uses a theoretical framework to produce spatial maps of the risk of poppy cultivation in Afghanistan, but do not formalize the relationship to actual cultivation. We complement these approaches by demonstrating the ability to pair our high-resolution maps with other freely-available grid-level data sets, to gain insight on socioeconomic conditions at a much more granular level. To our knowledge, this is the first application in which opium cultivation maps have been combined with grid-level data for this purpose.

3 METHOD

Our analysis proceeds in several steps that are guided by knowledge of characteristics of the opium poppy crop, including growing seasons and spectral properties, summarized from related work (see Section 2) in Table 1. The classification approach relies on the premise that major crops have different crop cycles and unique spectral properties [28, 53, 54, 67]. First, we use information from vegetation indices to derive optimal satellite imagery acquisition dates. Then, with acquired imagery before and after crops are harvested, we use an unsupervised clustering approach on selected training regions, to separate the pixels into suitable clusters. We identify the cluster corresponding to opium poppy using known crop characteristics. Finally, we fit the fitted model to the entire study area to obtain poppy cultivation maps. Additionally, we combine these derived maps with other publicly-available grid-level data set to investigate the socioeconomic characteristics surrounding cultivation. A more detailed description of our data and methodology is as follows:

3.1 Study Area

Our study area is Afghanistan, which accounts for 70–90% of the world's supply of illicit opium. Afghanistan has a land area of 65.29 million hectares, of which an estimated 12% is agricultural land [4]. Our analysis focuses on these agricultural areas. Afghanistan is divided into 32 provinces and 398 districts, and 195 have recorded some opium poppy cultivation in the last 5 years with available district-level data (2017–2021). To evaluate the efficacy of our method, we focus on the top poppy-producing regions in Afghanistan, specifically districts belonging to the top quartile of districts with poppy cultivation (by acreage; Figure 1A). In 2019, 2020, and 2021, these corresponded to 91.4%, 93.0%, and 93.2% of total opium poppy cultivation, respectively.

We analyze three growing seasons, from 2019 to 2021. This data period was chosen since 2019 is the first year in which high-resolution surface reflectance imagery is available for Afghanistan (see Section 3.2), and 2021 is the last year in which aggregated district-level cultivation statistics, which we use to evaluate our results, are available. Our method is easily extendable to later years (see Section 5). We analyze the main growing season, which begins in the Winter and ends in Spring/Summer.

3.2 Remote Sensing Data

Sentinel-2 Optical Data. Sentinel-2 is an Earth observation mission operated by the European Space Agency. It systematically acquires optical imagery at high spatial resolution (10 m to 60 m) over land and coastal waters. Images contain 12 spectral bands: four bands (visible and NIR) at 10 m, six bands (red edge and SWIR) at 20 m, and two bands (atmospheric) at 60 m spatial resolution. It is a constellation with two satellites; the revisit frequency of each satellite is 10 days and the combined constellation revisit is 5 days. Compared to other earlier satellites such as Landsat 7 and 8, Sentinel-2 offers a higher resolution with shorter revisit periods. Data are made publicly available by the European Space Agency, and are easily accessible on Google Earth Engine (https://developers.google.com/earth-engine/datasets/catalog/COPERNICUS_S2_SR_HARMONIZED), requiring only a browser and a straightforward application process to gain access. Level-2A orthorectified atmospherically corrected surface reflectance imagery are available from 2017, but are only available for Afghanistan from 2019. Optical satellite data were corrected for cloud cover using Sentinel-2: Cloud Probability data (https://developers.google.com/earth-engine/datasets/catalog/COPERNICUS_S2_CLOUD_PROBABILITY). These data are released by the European Space Agency to accompany the Sentinel-2 imagery. Each 10 m pixel has an estimated probability that the pixel is cloudy. We filter for cloud and cloud shadow components using standard recommended procedures³ that identify clouds using a threshold on the cloud probability, and nearby dark pixels using the near infrared (NIR) band.

MODIS Vegetation Indices. The normalized difference vegetation index (NDVI) is computed from the NIR and red spectral bands, as $NDVI = \frac{NIR - Red}{NIR + Red}$, and measures the amount of green vegetation. NDVI values are between -1 and 1, where values close to 1 indicate dense vegetation, values close to zero are urban areas, and negative values indicate clouds and snow. The Moderate Resolution Imaging Spectroradiometer (MODIS), launched by NASA in 1999, is a satellite-based sensor used for earth and climate measurements. The MODIS vegetation indices are a data product released at 250 m resolution at 16-day intervals. These are derived from composite products, and contain a representative NDVI value for the 16-day period, selected based on data quality and cloud cover [23]. Data are available on Google Earth Engine from 2000 to the present day (<https://>

³<https://developers.google.com/earth-engine/tutorials/community/sentinel-2-s2cloudless>. Several input parameters are required: we use CLOUD_FILTER = 50, CLD_PRB_THRESH = 70, NIR_DRK_THRESH = 0.2, CLD_PRJ_DIST = 5, and BUFFER = 50.

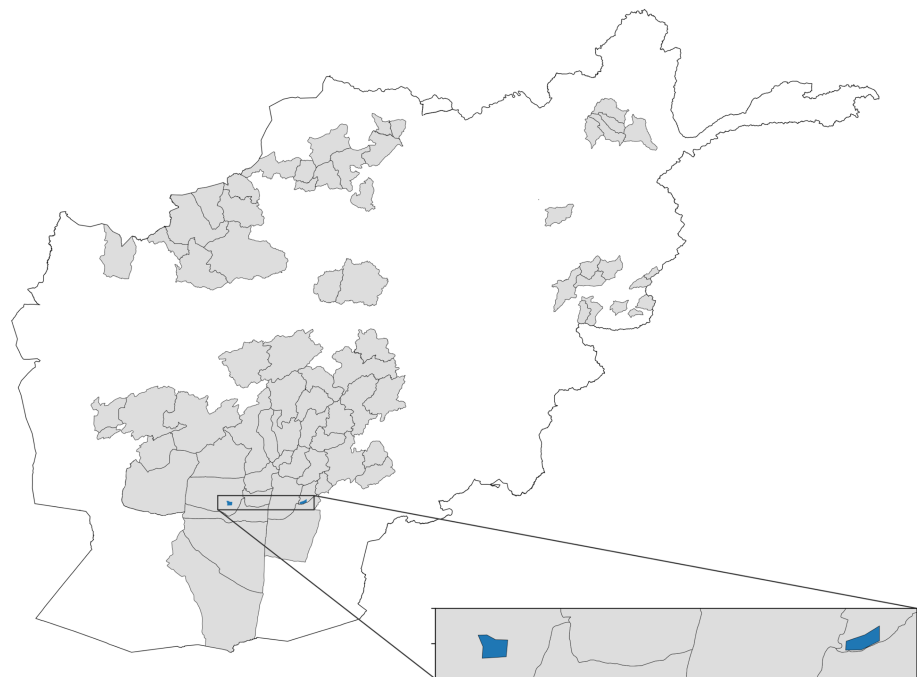
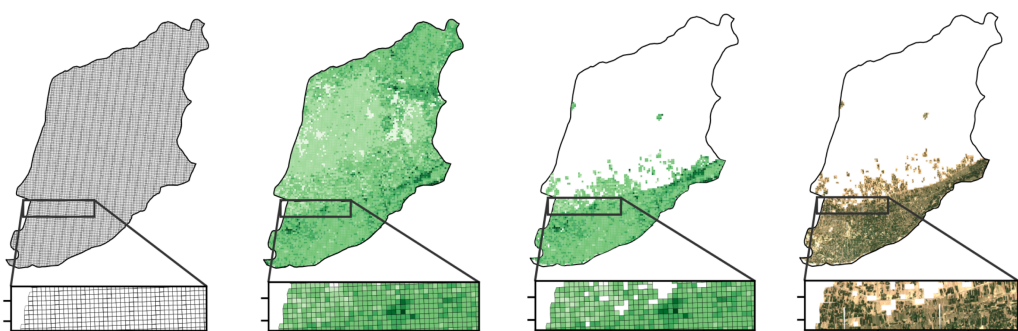
A**B**

Fig. 1. A: Map of Afghanistan. Districts in the top quartile of cultivation in 2019 are highlighted in gray. In blue are regions within the districts of Nad Ali (Helmand province) and Zhari (Kandahar province), from which model training data was extracted. B. Illustration of the process of estimating the optimal image acquisition dates in Zhari district (the district containing the second blue patch) in 2019. From left to right: first panel shows 250 m tiles covering the study area. Second panel shows peak MODIS NDVI dates, which we define to be the optimal pre-harvest date for image acquisition. Here, the lightest green corresponds to February 12, 2019, and the darkest corresponds to June 10, 2019. Third panel shows the same figure after applying the crop mask. Last panel shows pre-harvest Sentinel-2 imagery acquired at the modal optimal pre-harvest date over each 50 km grid cell; in this case, the entire region falls in the same 50 km grid square, with modal pre-harvest date April 7, 2019.

developers.google.com/earth-engine/datasets/catalog/MODIS_061_MOD13Q1). We use these vegetation indices to estimate optimal image acquisition periods.

Copernicus Global Land Cover. The Copernicus Global Land Cover Layer is a data product at 100 m resolution that classifies the earth's land area into different land use categories (e.g., urban, forest, and crops). Measurements come from PROBA-V, a satellite launched by the European Space Agency to monitor land cover and vegetation. Annual data are available from 2015 to 2019 (https://developers.google.com/earth-engine/datasets/catalog/COPERNICUS_Landcover_100m_Proba-V-C3_Global); we use data from 2019 to select likely crop areas. This data set has a discrete_classification band containing the land cover classification, containing 13 categories (with additional subcategories for some categories) including "Shrubs", "Urban / built up", "Cultivated and managed vegetation / agriculture", "Moss and lichen", "Oceans and seas." We use the category for cultivated and managed vegetation / agriculture (discrete_classification = 40). The data also has a discrete_classification-proba band, indicating the quality of the discrete classification, specifically a classification probability. We use a cutoff of 60% to designate as crop areas; from visually observing Sentinel-2 imagery, this cutoff sufficiently isolates barren land from cultivated land, while retaining edge pixels at the boundaries of crop areas.

3.3 Image Extraction and Processing

Existing work has established the importance of acquiring satellite imagery during appropriate periods in the crop cycle, in particular pre-harvest, close to the peak in vegetation activity, and post-harvest, after crops have been harvested [28, 47, 53, 54]. These time periods are when there are significant visual differences between opium poppy and other crops (primarily, wheat), as summarized in Table 1. However, to our knowledge, existing methods do not estimate these dates and acquire imagery in an automatic way, instead relying on manual calibration, for example, based on established crop calendars. In addition, the unsupervised methods reviewed in Section 2 rely only on pre-harvest imagery; post-harvest imagery is only used for manual visual interpretation by the UNODC. Our goal is to estimate optimal pre- and post-harvest dates, and acquire Sentinel-2 imagery automatically during both those periods, for use in our clustering algorithm.

Our method is illustrated in Figure 1B. We consider 250 m by 250 m tiles over the study area. For each tile, we find the date in which MODIS NDVI values peak during the main poppy growing season for each year (January to June). We call this the *optimal pre-harvest date*. We smooth these values over a 50 km grid, limiting the analysis to tiles containing agricultural land, using the following steps. (1) Mask the 250 m-tiled data set using the Copernicus Global Land Cover data set; specifically, remove tiles that do not contain any pixels (100 m resolution) with crops (described in Section 3.2). (2) In each 50 km grid cell, calculate the *modal pre-harvest date* among all qualifying 250 m tiles. This smoothing process corrects for tile-level discontinuities in peak NDVI dates, which could occur due to measurement error, even though we should expect vegetation growth to peak at similar times for neighboring 250 m tiles (see Appendix Figure A.1).

Given modal pre-harvest dates, we acquire Sentinel-2 imagery for all qualifying (with cropland) 250 m tiles using Google Earth Engine. For pre-harvest imagery, we use a 2-week window starting from the modal pre-harvest date. For post-harvest imagery, we use the period 30–45 days after the modal pre-harvest date. This 30–45 day time window was selected based on knowledge that the poppy harvesting process takes 8–12 days [55], and based on a visual exploration of different time-windows (15–30 days, 20–35 days, 25–30 days, 30–45 days, 35–50 days, and 40–55 days) on known poppy producing regions. This time window maximizes the likelihood of there being just two main competing crops, opium poppy and wheat, and for the crop characteristics in Table 1 to be most apparent in the pre-harvest and post-harvest periods. Example pre-harvest and post-harvest imagery is in Figures 4 and 5.

For each pixel, we calculate differences between the band values pre-harvest and post-harvest, for each of the 12 bands. We derive two additional variables: NDVI corresponding to the pre-harvest date (from the Sentinel imagery), and the number of days since the first day of the year that the pre-harvest imagery is captured; this encodes information about the crop cycle. We create a unified raster file with these 14 features for each pixel, for use in the unsupervised learning step. For the remaining analysis, we filter out pixels that have an NDVI value of less than 0.4 during the pre-harvest period. This is done to ensure an even more precise selection of regions likely corresponding cropland at the 10 m-pixel level.

3.4 Unsupervised Learning

With the assembled raster files with 14 features for each year, we use a pixel-level, unsupervised k -means clustering approach. We fit separate models for each year. For each model, we use data from two known poppy growing regions in Afghanistan, in the districts of Nad Ali and Zhari, shown in Figure 1A. We chose these areas because they are historically known to be poppy-growing regions, and have a known crop mix. Selecting these areas yields clusters that accurately and sufficiently isolate poppy from other competing crops, and allows us to visually examine model performance in a tractable manner.

The k -means algorithm requires the number of clusters (k) as an input. We set k to 3, since the major crops in our selected training area, during the image acquisition period, are wheat and poppy. The third class is a miscellaneous category reserved for other potentially agricultural pixels that are not wheat or poppy, for example, field boundaries, any other crops, non-crop pixels that were not filtered out in our pre-processing steps, such as tracks and paths. We use the Python scikit-learn implementation of k -means with default hyperparameters, with the exception of “init”, which we set to “random” (more details in Appendix B).

3.5 Identifying the Cluster Corresponding to Opium Poppy

To determine which of the three fitted clusters in the training region are most likely to be opium poppy, we use pre-harvest NDVI values, as well as a visual examination of RGB images, both pre-harvest and post-harvest. This is guided by the information summarized in Table 1. Specifically, we expect pixels corresponding to wheat to have the highest NDVI values, closer to 0.8. [60] employs a similar method, using individual NDVI values; here, we use the distribution of NDVI values (Section 4.1). The visual appearance of poppy pre-harvest should be a brighter green than wheat, while post-harvest, we should see lighter colors for poppy, indicating an earlier harvest, and plowed fields. After identifying the cluster number most likely corresponding to poppy in the training regions, we fit the fitted model to data in all districts. We repeat this process for each year.

We note that there is existing work on unsupervised crop type mapping that selects a different number of clusters for different geographic regions, based on the known crop mix (number of major crops + 1) [62]. In our case, we are constrained by the lack of reliable crop mix data on at a fine enough geographic scale (district-level, for example). However, given that our analysis is limited to regions with higher levels of poppy cultivation, and using our method of acquiring images based on crop cycles, the likelihood of there being two only two main crops, wheat, and poppy, are maximized (more details in Section 4.1). Using a larger value of k , like $k = 5$, produces clusters that look similar (Appendix Figure A.2). We also experimented with unsupervised methods other than k -means, such as GMMs, but these have poorer performance (Appendix Figure A.3).

3.6 Evaluating Clustering Accuracy

Ground truth data of cultivation at a field-level are not available, but we evaluate the accuracy of our results quantitatively using aggregated district-level total cultivation area, and qualitatively

through visual inspection. For the former, we sum the number of pixels corresponding to the identified poppy cluster for each year, and convert this to the number of hectares at a district level. We compare these against the “ground truth” district-level estimates as released by the UNODC. To qualitatively verify our model predictions, we visually inspect the RGB bands of the Sentinel-2 imagery at the derived optimal dates in which imagery was acquired, to evaluate if they are consistent with our expectations. Needless to say, this manual verification method is limited to a small number of examples. We select these examples strategically, including examples in the training areas, other districts where aggregated estimates show a good correspondence, over-prediction, as well as under-prediction compared to UNODC estimates.

3.7 Combining with other Grid-Level Data Sets

We combine the generated opium poppy maps with auxiliary grid-level data sets using spatial joins, to gain insight to the socioeconomic conditions surrounding poppy cultivation. We use six relevant secondary data sets, involving travel time to urban center, healthcare accessibility, infant mortality, years of schooling, relative wealth index (RWI), and HDI. These data range from 250 meter to 10 kilometer resolution. To best match the time frame available for these auxiliary data sets, we use cultivation maps for 2019. For each grid cell in the secondary data set, we compute the proportion of pixels with poppy cultivation, and the proportion of pixels with other agriculture, where other agriculture corresponds to areas classified by the k -means algorithm as being in the two non-poppy clusters. Then, among all grid cells with any agriculture (poppy or others), we compare the distributions of the various socioeconomic variables for grid cells with any amount of poppy cultivation, and those with none, that is, only other crops.

A more detailed description of each data set is as follows: (1) Travel time (in minutes) to the nearest urban center [64] is estimated at 1 kilometer resolution, as of 2015. It is created as part of the Malaria Atlas Project, and is available at <https://data.malariaatlas.org/maps>. This can be interpreted as a measure of how remote a location is. (2) The healthcare accessibility data set, also created by the Malaria Atlas Project [63], contains predictions for land-based travel time (in minutes) to the nearest hospital or clinic at 1 kilometer resolution, as of 2019. It is available at https://developers.google.com/earth-engine/datasets/catalog/Oxford_MAP_accessibility_to_healthcare_2019. (3) For infant (under 1) mortality, predictions are available for the number of under-1 deaths per 1,000 live births, at a 5 kilometer resolution, yearly from 2000–2017 [14]. These are available at <http://ghdx.healthdata.org/record/ihme-data/lmic-under5-mortality-rate-geospatial-estimates-2000--2017>, and we use data from 2017. (4) Years of schooling for males and females are available at a 5 kilometer grid level, yearly for 2000–2017 [39], at <http://ghdx.healthdata.org/record/ihme-data/lmic-education-geospatial-estimates-2000--2017>. We use data for mean years of schooling among those aged 15–49 disaggregated by sex, in 2017. (5) Relative wealth estimates, as of approximately 2018, are available at a 2.4 kilometer resolution [15]. This is a measure of household asset wealth relative to others in the same country. (6) Global high resolution estimates of the United Nations HDI are available at a 10 kilometer grid level in 2019 [44], at <https://www.mosaiks.org/hdi>. The HDI is a multidimensional measure of development, incorporating information about not only income, but also education and health.

In addition, to provide background on the physical characteristics of poppy-growing regions versus areas with exclusively other agriculture, we characterize their geographic and climatic conditions using a similar methodology. Here, we use data on elevation, precipitation, and temperature. Elevation data, based on radar measurements and released by NASA [25], are available at 90 meter resolution at https://developers.google.com/earth-engine/datasets/catalog/CGIAR_SRTM90_V4. Monthly precipitation and temperature, derived from observations and regional

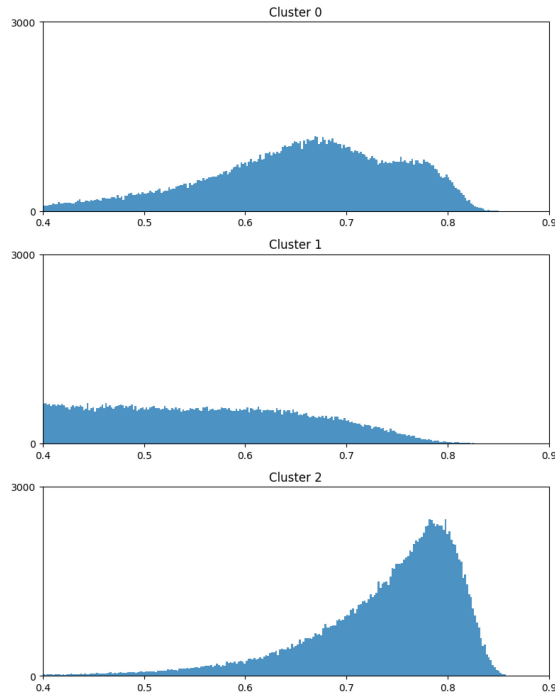


Fig. 2. Distribution of NDVI values from pre-harvest pixels of the model training region, by fitted cluster number, in 2019. The distribution for cluster 2 peaks at around 0.8 and has relatively smaller variance, suggesting that this cluster is likely to correspond to wheat. Cluster 0 has a peak at around 0.67, likely corresponding to poppy. There is also a smaller peak closer to 0.8, suggesting the presence of some wheat pixels. Cluster 1 has a large range of smaller NDVI values with no obvious peaks, likely corresponding to the miscellaneous category. Corresponding NDVI profiles for the three clusters in 2020 and 2021 are in Appendix Figure A.5 and show similar sets of profiles.

reanalysis [1], are available at 4 kilometer resolution from 1958 to 2022 at https://developers.google.com/earth-engine/datasets/catalog/IDAHO_EPSCOR_TERRACLIMATE. We use mean monthly values in 2019.

4 RESULTS

4.1 Identifying Poppy Clusters

Figure 2 displays the distributions of NDVI values in model training regions, for pixels classified as being in each of the three fitted clusters for 2019. In Figure 2, we see that the distribution of NDVI values for pixels belonging to cluster 2 peaks at around 0.8 and has relatively smaller variance. This suggests that this cluster is likely to correspond to wheat. On the other hand, cluster 0 has a peak at 0.67 and higher variance, which is consistent with the expectation that NDVI values for poppy should increase more gradually and peak at the 0.6–0.7 range. We also see values closer to 0.8, which suggest that there might be pixels corresponding to wheat that are misclassified. In this case, cluster 1 is likely to correspond to the miscellaneous category, with a large range of NDVI values with no obvious peaks. A point to note is that in general, some variability in NDVI values is expected, since image acquisition dates do not correspond perfectly to pre-harvest periods for

every pixel.⁴ Corresponding NDVI profiles for the three clusters in 2020 and 2021 are in Appendix Figure A.5, with similar results. In the 3 years, we identify clusters 0, 1, and 2, respectively, to be the clusters corresponding to poppy.

Additionally, we visually inspect the results in the model training region to verify that these clusters are correctly chosen. Example imagery from 2020 for Nad Ali and Zhari districts that are part of the training region are in the first two rows of Figure 4. In the first row, the visual characteristics described in Table 1 are obvious. In Panel A (pre-harvest) we see areas that are darker green, likely corresponding to wheat, and areas that are a brighter green, likely corresponding to poppy. In Panel B, we see that many of the brighter green areas are now beige, consistent with poppy fields being plowed after harvest. Many of the darker green areas are now a brown shade, indicating the ripening of wheat. Panel C highlights areas corresponding to cluster 0, which is the poppy cluster as identified using the NDVI profiles. In this case, we see many poppy fields being correctly classified as poppy. Many of the wheat areas, particularly on the right side of the image, are correctly not classified as poppy. However, a good number of wheat fields are also misclassified, for example, in the area just below reference point A, as well as to the top right of reference point B. This is likely because the wheat has ripened sufficiently to be mistaken as poppy.

Similar patterns can be observed in Zhari district in the second row—most of the poppy pixels are correctly classified, while wheat pixels above reference point A and to the left of reference point B are misclassified as poppy. In this district, we also note the presence of other crops beyond poppy and wheat. For example, there is a different crop to the top right of reference point C, that has not ripened in the pre-harvest period. In the post-harvest period, it is much greener and closer to ripening. This crop has a different crop cycle, and the careful selection of image acquisition dates results in these pixels correctly not being classified as poppy. This point is true more generally in other districts with different crop mixes: the selection of image acquisition dates maximizes the likelihood of there being the two main crops of wheat and poppy acquired at the correct stages of the growing cycle, particularly in the regions of interest with larger amounts of poppy cultivation. This validates our decision to focus on the two main crops of poppy and wheat, and justifies the selection of $k = 3$ for the number of clusters.

4.2 Comparing with Aggregate Statistics

Figure 3 plots the aggregated district-level acreage estimates from our method against UNODC estimates for 2019, 2020, and 2021, respectively, for districts in the top quartile of cultivation in each year. We see a strong correlation between our estimates and UNODC estimates, with a Pearson correlation correlation of 0.777, 0.758, and 0.814 for 2019, 2020, and 2021, respectively. For all three years combined, the correlation coefficient is 0.771.⁵ We see some over-prediction, particularly for the two top-producing districts, which we investigate further through visual examination in Section 4.3.

In these figures, we note that model performance is much more variable in districts with lower levels of cultivation (leftmost data points in the figures). This is likely because in these districts, the crop mixes are much more heterogeneous, with opium poppy being only a minor crop. Computed optimal acquisition dates may correspond to other major crops that have a different growing cycle than opium poppy, and so imagery acquired may not capture opium poppy at the right stages of

⁴As a secondary validation of the results, we produce a standard t-SNE plot [59] showing the separation between clusters (Appendix Figure A.4).

⁵ $R^2 = 0.59$. For comparison, the prediction accuracy (measured using R^2) for other sustainable development outcomes using satellite imagery and machine learning are around 0.65 for village/district-level asset wealth, and 0.42 for plot-level smallholder yields [13].

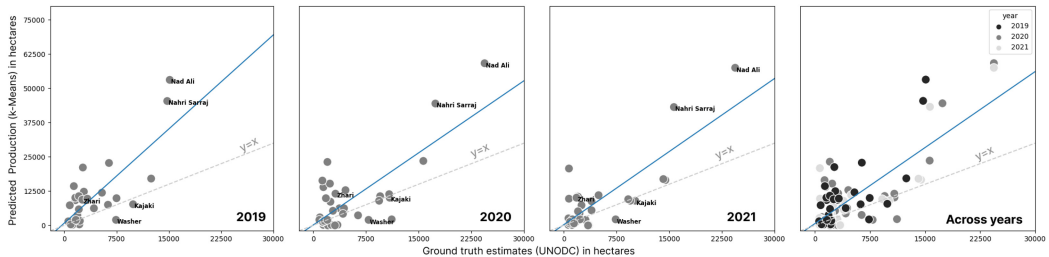


Fig. 3. Aggregated predicted production vs. UNODC district-level estimates, for districts in the top quartile from 2019 to 2021. Points marked with text labels are district names for districts with example imagery in Figure 4. The blue line is the best fit line, and the dashed line is the 45-degree line. Pearson correlation coefficients for each of the panels are 0.777, 0.758, 0.814, and 0.771, respectively.

growth. There might also be the presence of other crops that are misclassified as poppy. We might thus expect a deterioration of model performance in districts with small amounts of opium poppy cultivation.

4.3 Visual Examination

To further verify our model predictions and to understand the reasons for over-prediction and under-prediction, we visually inspect additional clustering results in non-training areas, using RGB imagery for both the pre-harvest and post-harvest dates. Rows 3–5 in Figure 4 show predicted poppy pixels in 2020, for examples, in three different districts, and Figure 5 shows model performance over time using the same area as in row 4 of Figure 4.

In districts where our method over-predicts (rows 1–3), we see that our method misclassifies some likely wheat pixels as poppy. The first two rows were described in Section 4.1, where we saw wheat pixels being classified as poppy because they had ripened in the post-harvest imagery. In the third row (Nahri Sarraj), we see a potential explanation for this behavior: there are some poppy fields here that have not been plowed in the post-harvest imagery, and resemble the ripened wheat pixels in the first two rows. Reference point A shows poppy fields that were plowed as expected, but poppy fields around reference point B are not plowed, likely because the post-harvest imagery was obtained too early. All of these pixels are in the poppy cluster. Such measurement errors in the post-harvest date are one potential reason for our model’s inability to distinguish between poppy and wheat pixels.

In Kajaki district (row 4), our predictions are roughly consistent with UNODC estimates (the ratio of $\frac{\text{model estimates}}{\text{UNODC estimates}}$ is 0.94). Here, there is a sufficient distinction in the growth stages of poppy and wheat, such that the model correctly distinguishes between them. For example, the areas around reference point A exhibit the visual characteristics of being poppy, and are correctly identified as such; the areas to the left of reference point B exhibit the visual characteristics of being wheat, and are correctly identified as not being poppy. Finally in Washer district (row 5), where there is under-prediction, we see that the pre-harvest and post-harvest imagery is virtually identical. In this case, errors in image acquisition dates result in an inability to correctly classify many poppy pixels.

Finally, we find that the prediction behavior of our method is consistent across time, despite variability in the suitability of image acquisition dates (Figure 5). Of the 3 years in the figure, the quality of imagery is the best in 2019, where bright green areas are obviously beige by the post-harvest period, indicating opium poppy fields. The model correctly identifies these areas as poppy. In 2020, in the post-harvest imagery, not all poppy fields have been plowed, but the model

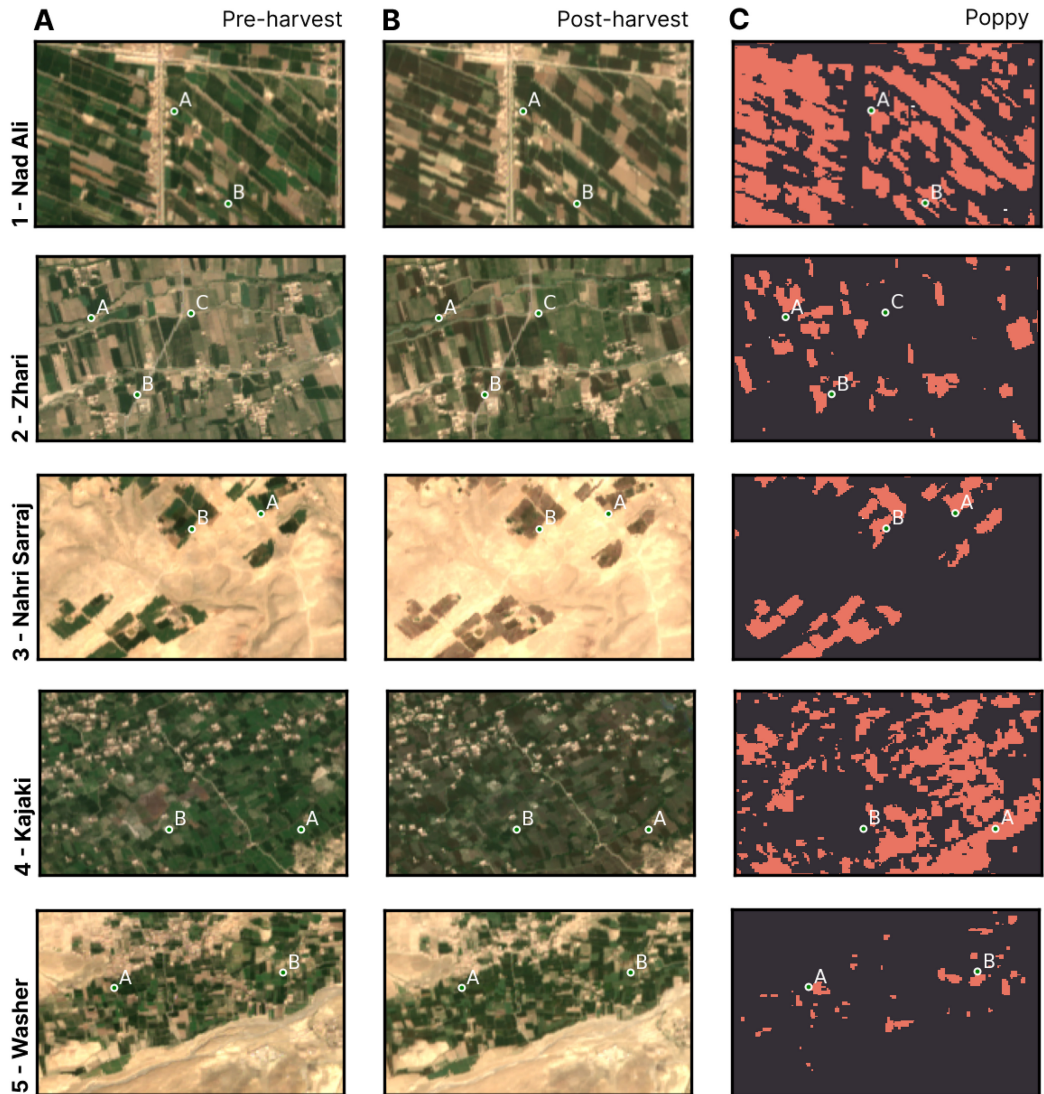


Fig. 4. Examples of clustering results from training (rows 1–2) and non-training (rows 3–5) regions in 2020. The points marked A, B, and C are reference points; more details in main text. Column A displays pre-harvest imagery, B displays post-harvest imagery, and C displays pixels in the poppy cluster in pink. Rows 1–3 are examples from regions with over-prediction relative to UNODC estimates; row 4 is from a region with predictions similar to UNODC estimates; row 5 is from a region with under-prediction.

is still able to correctly identify many of them. We can also see our method's ability to respond to changing cultivation patterns over the years. Comparing the area just to the right of reference point B across the 3 years, we see that in 2019 this is likely to be a poppy field. In 2020 and 2021, the darker green appearance in both pre-harvest and post-harvest imagery indicate that it is more likely to be wheat. Our model seems to be correctly picking up on this pattern, identifying the area as being poppy-growing in 2019 and not poppy-growing in 2020 and 2021.

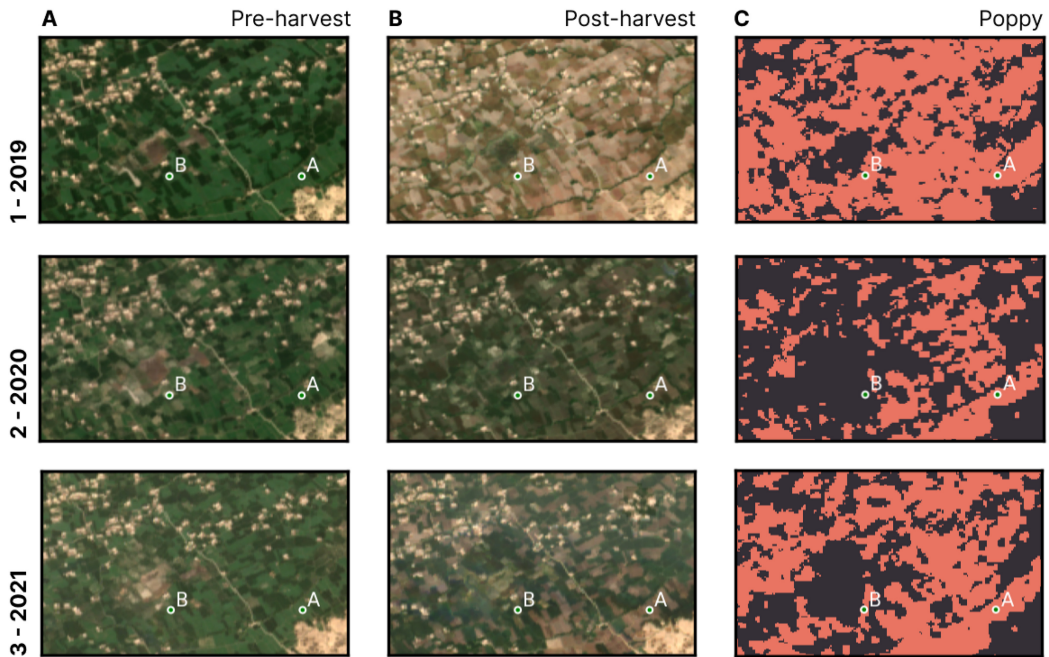


Fig. 5. Model performance across years 2019 (row 1) to 2021 (row 3). The points marked A and B are reference points; more details in main text. Column A displays pre-harvest imagery, B displays post-harvest imagery, and C displays pixels in the poppy cluster in pink.

To summarize, when the pre-harvest and post-harvest imagery exhibits the visual characteristics described in Table 1, and capture poppy and wheat in sufficiently distinct growth stages, the model is likely to correctly classify poppy pixels. When the post-harvest imagery is timed imperfectly, poppy is sometimes not classified as such when captured too early, while wheat is misclassified as poppy, particularly when it has ripened sufficiently by the post-harvest image acquisition date. Instead of using a fixed post-harvest acquisition date of 30–45 days after the modal pre-harvest date, a more fine-tuned, 50 km cell-level approach might improve the accuracy of the model.

4.4 Socioeconomic Conditions Surrounding Cultivation

To first provide context on the differences between poppy-growing and non-growing regions, we characterize poppy-growing areas and areas with exclusively other agriculture based on their physical characteristics of elevation, precipitation, and temperature (Appendix Figure A.6). Grid cells with any poppy cultivation tend to be at lower elevations (mean of 856 m versus 1,193 m for grid cells with only non-poppy agriculture). This is consistent with opium poppy most typically being grown on large, flat plots of land, rather than on terraced fields [7]. Grid cells with poppy cultivation tend to also experience lower monthly precipitation (mean of 19.4 mm versus 30.9 mm for grid cells with non-poppy agriculture) and higher minimum and maximum temperature (mean maximum temperature of 28.1°C versus 23.6°C for grid cells with non-poppy agriculture) than grid cells with non-poppy agriculture. The opium poppy crop is frost-sensitive and requires dry, warm weather during ripening [29]. In addition, it requires less water than competing crops such as wheat, and farmers often use irrigation systems, explaining these observations.

Next, we consider how remote these areas that are physically suited to opium poppy cultivation are, compared to other agricultural areas. Using data on travel times to the nearest urban

center, we find that compared to agricultural areas with no poppy cultivation, grid cells with any amount of poppy cultivation have shorter travel times to urban areas (mean of 193 minutes versus 237 minutes for other agricultural areas). Related to this, poppy-growing grid cells have on average better access (shorter travel times) to healthcare facilities (mean of 89 minutes versus 225 minutes for other agricultural areas). On the other hand, poppy-growing areas have higher infant mortality (mean of 2.6 under-1 deaths per 1,000 versus 1.50 for other agricultural areas) and lower years of schooling (males: mean of 5.47 years for poppy-growing areas versus 7.55 for other agricultural areas; females: 2.08 years versus 2.80 for other agricultural areas). Boxplots showing the distribution of these variables are in Figure 6. Finally, grid cells with any amount of poppy cultivation have slightly lower scores both on the RWI (mean of -0.46 for poppy-growing versus -0.40 for non-poppy agricultural areas) and the HDI (mean of 0.38 for poppy-growing versus 0.40 for non-poppy agricultural areas) (Figure 7). Statistical tests for differences in means between the no poppy and any poppy groups are significant in all cases ($P < 0.001$).

In general, the literature points to poppy-cultivating areas as having more insecurity and less government presence, lower levels of development, and associated indicators such as access to schools and healthcare facilities [29]. Our results are largely consistent with these predictions. The finding that areas with poppy cultivation have shorter travel times to urban centers is interesting and merits further discussion. There are conflicting accounts from the literature: [29] suggests that lack of accessibility contributes to socio-economic vulnerability, which is a risk factor for opium poppy cultivation. Yet [65] finds that infrastructure development in the form of road construction leads to more opium poppy cultivation. Here, our results are consistent with the latter argument. The result on accessibility to healthcare follows from this result: accessibility to healthcare is a function of two quantities: transportation infrastructure and the availability of healthcare. We might expect poorer healthcare availability in poppy-growing regions, consistent with more insecurity and a lower level of development—yet likely because of the better overall transportation infrastructure, we observe shorter travel times to healthcare facilities in poppy-growing areas.

Another interesting finding is that the shorter travel time to a healthcare facility does not translate to lower infant mortality (Figure 6B). This could be because of numerous other barriers to receiving care, such as poverty, low literacy rates, lack of female healthcare providers, insecure travel, and an inability of women to travel without a male escort [6]. These factors might be exacerbated in opium-cultivating areas; for example, constraints on the movement of women are particularly acute in Taliban-controlled, opium-cultivating areas [36]. As a result, lower travel times do not necessarily translate to women and infants receiving appropriate care. One important caveat, however, is that while the other auxiliary data sets used in Figure 6 are geographically complete, the infant mortality data set is missing estimates in more rural areas due to availability of data; this results in about 15% of agricultural pixels being dropped from the analysis. Additionally, for the mortality and education outcomes, we use the most recent year of data available, 2017, paired with opium poppy predictions for 2019. While more recent data are not available, these socioeconomic outcomes tend to change slowly across years.

In terms of development indices, poppy-growing areas score slightly worse on two such indices, RWI, and HDI. The RWI data set predicts asset-based relative household wealth using high-resolution satellite imagery, data from mobile phone networks, topographic maps, and Facebook connectivity data. The HDI data set predicts HDI as defined by the United Nations Development Program (UNDP)—an average of achievements in health, education, and standard of living [48]—using satellite imagery. While there are limitations associated with both these data sets, in particular prediction errors and geographical incompleteness due to data availability, they point to the same conclusion, which is that poppy-growing areas have lower levels of wealth and

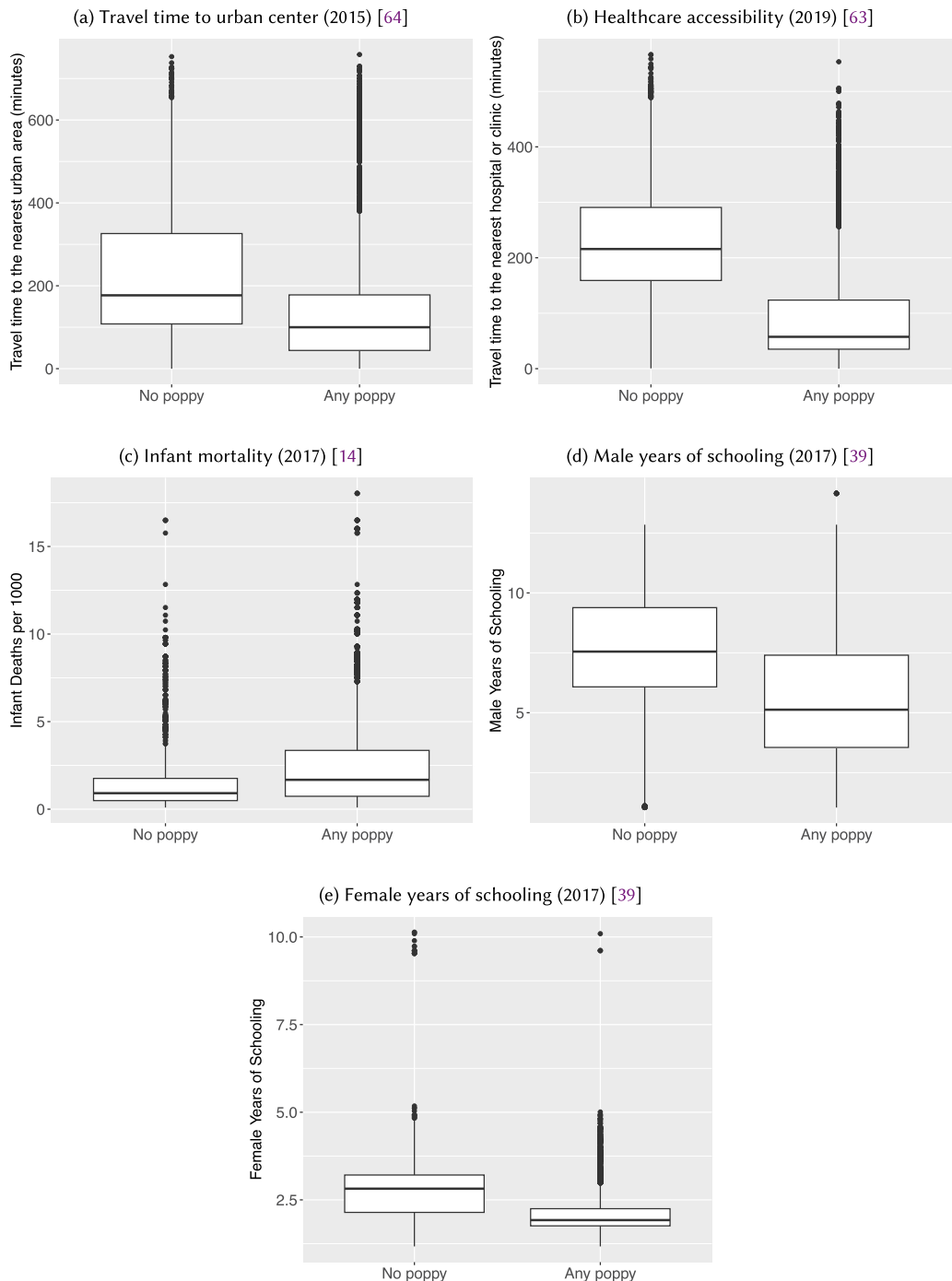


Fig. 6. Distribution of socioeconomic outcomes in agricultural grid cells that are classified as having no poppy cultivation in 2019, versus those that have any amount of poppy cultivation.

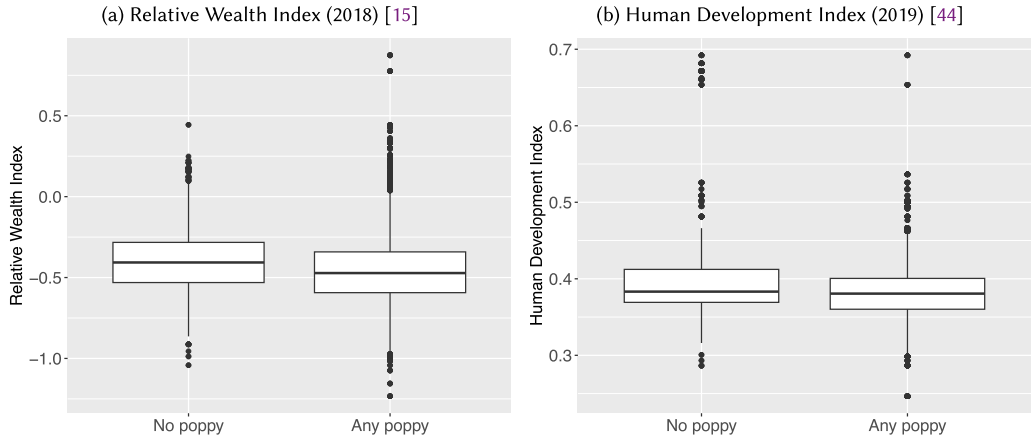


Fig. 7. Development indices in agricultural grid cells that are classified as having no poppy cultivation in 2019, versus those that have any amount of poppy cultivation.

development. The finding on wealth might be surprising given that opium poppy is seen as a lucrative cash crop; a prior expectation might be that poppy-growing areas are wealthier than non-poppy growing areas. This result has two potential explanations. First, there might be selection into poppy cultivation. Opium poppy is described as a crop that farmers turn to when other crops fail [20]. Hence, agricultural areas that continue to cultivate exclusively other crops may be economically better off. Second, the measure of wealth is based on asset ownership. While opium poppy cultivation does provide short-term income, it might not be invested into assets that would improve longer-term outcomes. This is supported by surveys that indicate that the income that farmers earn is used primarily to cover daily necessities such as food and medical expenses, as opposed to savings and longer-term investments [55].

A final point to note is that our analysis does not claim a causal effect of opium poppy cultivation on these various indicators, or vice versa. Establishing such causal relationships is beyond the scope of the current analysis but is an important topic for future work. On a related note, neither is our goal is to suggest that our estimates for poppy cultivation should be used as a proxy for the socioeconomic variables that we have analyzed, or vice versa—our objective is to provide quantitative evidence on the differences between poppy-growing and non-poppy growing regions, and we demonstrate how this is made possible with the granular maps of poppy cultivation that we produce.

5 DISCUSSION

We have developed an unsupervised approach to map opium poppy cultivation in Afghanistan, producing the first freely available maps at a 10 m resolution. Since ground truth data on cultivation at a similar resolution are unavailable, we evaluate the accuracy of our results using official district-level statistics, as well as by visual inspection. We find that for districts accounting for over 90% of total cultivation, aggregated estimates track official district-level estimates closely, although there are some inaccuracies. In particular, there is some over-estimation due to wheat being misclassified as poppy. Visual inspection of the imagery is largely consistent with expectations, and reveal some reasons behind these inaccuracies.

One source of the confusion between wheat and poppy is the error in estimating the appropriate timing of image acquisition windows. As we detail in Section 4, when post-harvest imagery is acquired too early, poppy is not classified as such, and when imagery is acquired too late, wheat is confused with poppy. One natural extension of our work would be to investigate methods to select the post-harvest acquisition date in a more data-driven manner, rather than using a fixed number of days after the pre-harvest acquisition dates. One caveat is that there might be an inherent difficulty in distinguishing these two crops, which may limit the effectiveness of any solution. This limitation is shared by other work that uses completely different data and methods; for example, [53] use both optical and synthetic aperture radar imagery with supervised classification approaches to classify wheat pixels, and document the same issue.

Despite some inaccuracies in the maps that we produce, we demonstrate that they remain useful in generating additional insight on accessibility, healthcare accessibility, education, infant mortality, and overall development. Some of our findings corroborate findings from other work: we find that agricultural areas that have any poppy cultivation have higher infant mortality and lower levels of schooling, compared to areas without poppy cultivation. Our fine-grained analysis reveals other surprising insights that would not be obvious from a more aggregated analysis. For example, poppy-growing areas have better healthcare accessibility, likely due to better transportation infrastructure. Related to this point, poppy-growing regions compared to areas with exclusively non-poppy agriculture have shorter travel times to urban centers, that is, by this metric are less remote, yet have lower levels of development. This stands in contrast to other work that describes accessibility as a necessary condition for many development targets [64], and that shows an empirical relationship between more remote locations and lower levels of development [21]. Despite being better connected to urban centers, poppy-growing regions have not appeared to have used this to their advantage in terms of overall development.

Our approach has several limitations. First, our methodology relies on some knowledge of crop characteristics, as well as a basic understanding of the crop mix. This knowledge was used in designing the image acquisition and clustering strategy, as well as to select training regions and identify the appropriate poppy cluster. The methodology works best when there are larger amounts of opium poppy cultivation and a smaller crop mix, as is observed in many high-growing districts. With smaller amounts of the opium poppy crop, chances are higher that computed image acquisition dates do not capture opium poppy at the right stages of growth, resulting in poorer model performance. These factors might limit the direct application of our method in different locations (countries) and over time. In the Afghanistan context, we show that training regions are generally stable over time, and our method transfers easily between years in our study period. However, large shocks such as the recent 2022 ban on opium poppy cultivation by the Taliban may drastically change the crop mix, necessitating changes to the methodology. In addition, validation of our predictions is limited by the lack of field-level ground truth data, and future work might investigate the possibility of collecting expert-based labels in a cost-effective yet accurate manner. Labeled data would significantly strengthen the evaluation of prediction performance, enabling the use of standard metrics commonly used in the remote sensing literature, such as overall accuracy and Kappa coefficients [3, 66]. In addition, the availability of labeled data would allow the development of a supervised model; while not the focus of our work, this is likely to yield more accurate predictions [62].

Next, our intention is to provide a low-cost, freely accessible means of generating granular maps of opium poppy cultivation, which can be used to study local phenomena over a wide geographical area. Our ideal audience would be researchers whose goal is to understand local conditions surrounding such illicit cultivation, and we have demonstrated the utility of our generated maps

for this purpose. As such, we have made all our code and maps publicly available (see Appendix B) so that they can be implemented easily. We acknowledge that depending on goals and budgetary concerns, our methods may not produce the most accurate or suitable maps available. For example, the UNODC places a much heavier emphasis on accurately computing aggregate totals in official statistics, and expends significant resources towards this end. They also invest heavily in visual interpretation (manual annotation) of imagery, which would be amenable to training a supervised model. A different goal might be to conduct a case study of a certain village or high-cultivation area; in this case a more suitable alternative may be to purchase high-resolution imagery, and either annotate the images manually, or develop an automatic classification method that has the highest accuracy for this geographical area.

An important consideration is the impact of the misclassification errors that were discussed in detail in Section 4, on downstream applications. In particular, estimates are much more variable in districts with smaller amounts of opium poppy cultivation, and wheat and poppy are sometimes confused, leading to both over-estimation and under-estimation. First, performance is likely to be poorer in applications that require the precise estimation of the amount of poppy cultivation at a very granular level. For instance, in our analysis using grid-level socioeconomic data, we focused on a binary classification of whether 1 km-grid cells have any poppy cultivation, rather than a continuous variable for the amount of poppy cultivation. This is because uncertainties in cultivation amounts, compounded with uncertainties in some of the socioeconomic variables, would result in relationships that are too noisy. Other potential ways to mitigate this issue would be to consider coarser grid cells, such as 10 km, or to limit the analysis to districts in which there is less known over- or under-estimation. Further, downstream applications that depend on accurately differentiating between wheat and poppy are likely to similarly suffer in performance. For example, it is possible to pair poppy cultivation maps with granular data on food insecurity [19]. However, food insecurity is affected by both wheat and poppy cultivation, potentially in different ways. Resulting conclusions might therefore be sensitive to the misclassification of wheat as poppy and vice versa. Like many prediction models, ours is not without error, and as these examples illustrate, a thoughtful consideration of their suitability for various downstream applications is essential.

Future work can address some of the above-mentioned sources of inaccuracies and limitations. More broadly, by making our methods and data publicly available, our work creates avenues for future work on the causes and consequences of opium poppy cultivation in Afghanistan, as well as the evaluation of development programs over multiple growing seasons. With the recent proliferation of granular grid-level data, there are many opportunities to pair these with cultivation maps to gain a deeper insight on local conditions. Some avenues that remain unexplored include climate and drought [1, 43], violence [51], and population [52]. One specific potential application is to accurately estimate the number of people involved in poppy cultivation. This has been described as “persistent knowledge gap” [55] – while the strength of our method is in the granularity of the data, it can be combined with granular population data and then aggregated to produce such statistics. In all these applications, it is worth reiterating that we are limited by the accuracy of the maps as well as the quality and availability of auxiliary data sets. Since many auxiliary data sets are designed for global coverage, estimates for Afghanistan may be less accurate or difficult to verify, due to the general poor data availability or quality in the country.

Further work can be done to see if and how our method transfers to other poppy-producing regions in the world, such as Myanmar. A careful investigation should be done to document if the same types of misclassification errors exist, and what their implications might be in these different contexts. We also hope that our approach to generating more fine-grained insight on illicit

cultivation in Afghanistan can inform work in understanding the local environments surrounding the cultivation of other illicit crops, such as coca. Coca cultivation is concentrated in South America, and like opium poppy, coca is not typically represented in more general crop-type mapping studies [8]. Producing coca cultivation maps based on timely, freely available data could facilitate research in these similarly challenging settings.

Finally, while satellite imagery creates new possibilities for understanding opium poppy cultivation, we recognize that there are ethical concerns associated with the use of such data, and have considered them carefully. Even though the use of satellite imagery for crop detection has become commonplace, it is important to be cautious about its applications in sensitive contexts. General frameworks for the ethical use of big data in development are discussed in more detail in [10, 38] and others. More closely related to our work, [11] addresses concerns and makes suggestions for the use of Sentinel-2 imagery in vulnerable, conflict settings. The granularity of our maps might be a cause for concern, especially since our approach is easily reproducible and thus has the potential to be misused. While our intention is for these maps to be used for research purposes, we consider the possibility that other bad actors could use this information for nefarious purposes. For several reasons, we assess this possibility to be remote.

First, the goal of these maps is to enable analysis on a large-scale, and its utility is not in targeting individual farmers. It is not possible to identify or locate individual farmers using our approach; we simply identify 10 m pixels that are likely to contain opium poppy crops. More importantly, key actors with an interest in opium poppy cultivation in Afghanistan are likely to already possess information that exceeds what remotely sensed data, and in particular publicly available remotely sensed data, are able to provide. For non-state actors (the Taliban, in particular), the location of poppy fields, particularly in the high-cultivation areas that we focus on, is already well-known. Each year, Taliban fighters have been known to participate in the labor-intensive harvest. They collect taxes from farmers after the harvest, and are involved in the subsequent heroin supply chain, including manufacturing and trafficking [56]. For these reasons, the information that the Taliban has on the opium industry almost certainly exceeds the information contained in our maps. Another concern may be that forces aligned with the government might use this information to target farmers that grow opium poppy. Again, we can expect these groups to have superior prior knowledge. In the past, the United States and other governments have spent billions of dollars on counter-narcotics efforts, some of them involving eradication of opium poppy fields using aerial spraying or physical destruction of the crop [49]. This required local knowledge and resources, making it unlikely that our maps, derived entirely from publicly available information, furnish any additional information.

For these reasons, we do not expect these maps to have unintended negative effects on the safety or privacy of farmers. Regardless, when possible, we take precautions to protect the privacy and welfare of farmers; for example, we only publish maps for the highest-producing quartile, where results are more robust.

To conclude, we have demonstrated how freely available satellite imagery can allow us to study poppy cultivation patterns in great detail. Our approach has several advantages over existing methods: it is based on timely, freely available data, uses only open-source software and code, and is easily scalable to a large geographical area. More broadly, we hope that our work can facilitate a better understanding of local characteristics surrounding illicit cultivation, and ultimately contribute to the design of effective development programs. While illicit crop cultivation is a local phenomenon, its implications are global, and a deeper understanding of their dynamics is crucial.

APPENDICES

A APPENDIX A: ADDITIONAL FIGURES

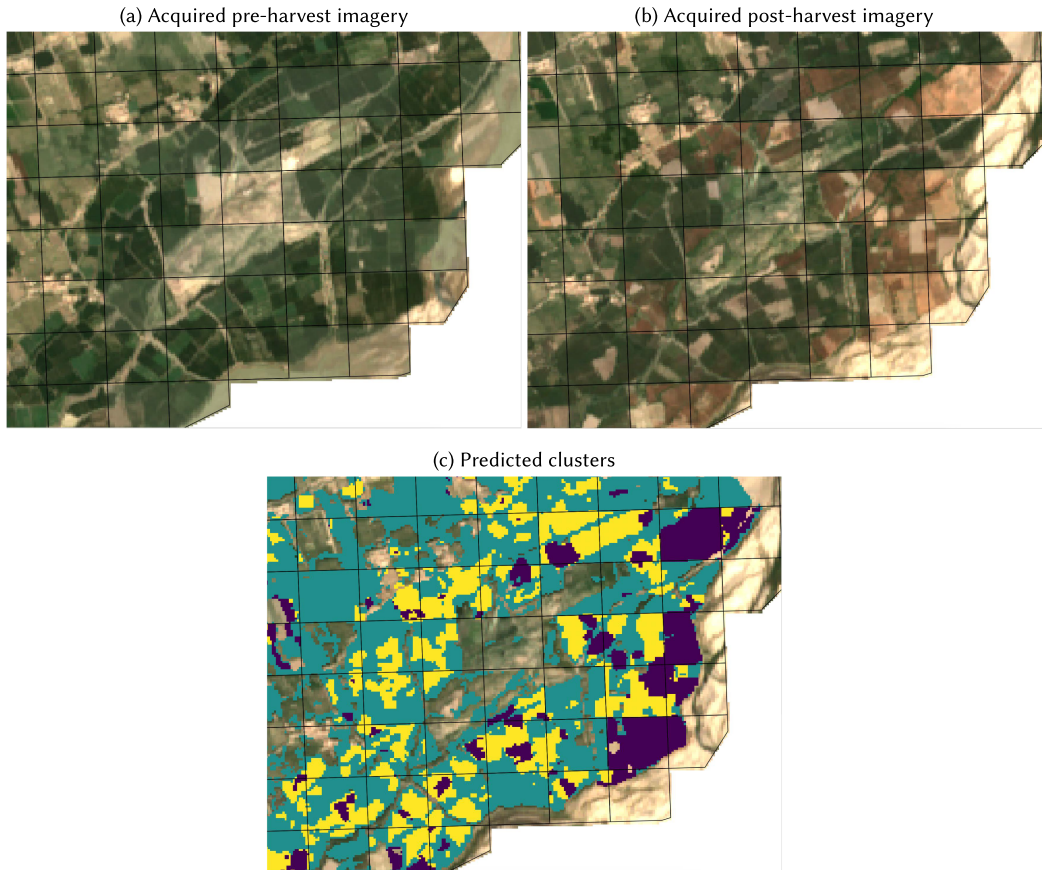


Fig. A.1. Tile-level discontinuities when using 250 m tiles to estimate acquisition dates. To determine optimal satellite imagery acquisition dates, we use a 50 km grid (Section 3.3). This corrects for tile-level discontinuities in estimated peak NDVI dates when a finer grid is used. Here, we use 250 m tiles on an example area in Zhari district to illustrate this point. (A) displays acquired pre-harvest imagery and (B) displays post-harvest imagery, where maximum NDVI was estimated at a 250 m tile-level (black boxes). The pre-harvest imagery is as we would expect. The post-harvest imagery; however, has noticeable discontinuities: in adjacent tiles, some fields are post-harvest, as intended, but some are so far post-harvest that wheat has been harvested as well. The discontinuities arise because in the pre-harvest imagery, consecutive 16-day periods for some tiles have very similar NDVI values, resulting in the algorithm selecting different periods for neighboring tiles. (C) displays clustering predictions: yellow is the expected poppy cluster. We see that the tile-level discontinuities persist, resulting in misclassification errors.

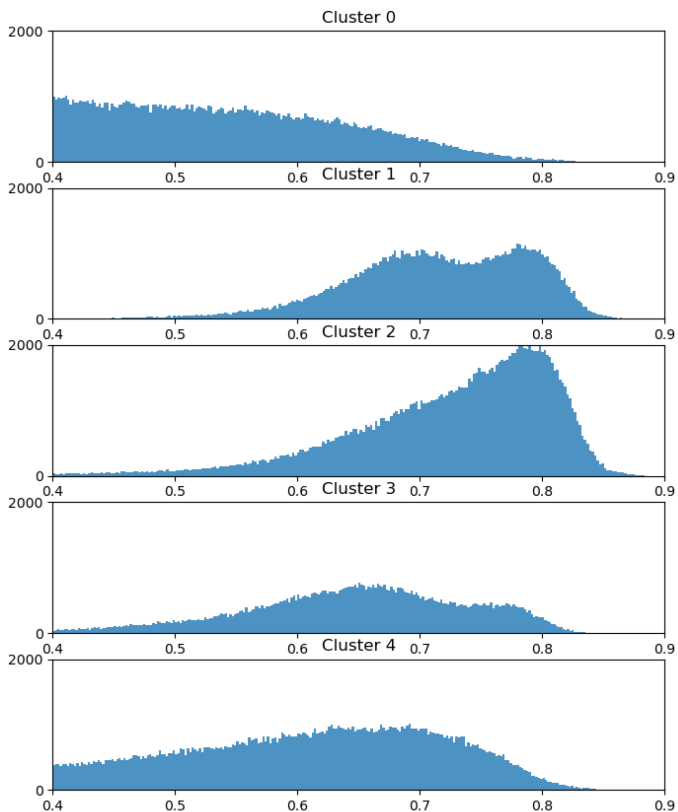


Fig. A.2. Distribution of NDVI values from pre-harvest pixels of the model training region, by fitted cluster number, in 2019, using k -means with $k = 5$. Here, we see poorer separation between the clusters, with wheat pixels (expected NDVI closer to 0.8) in clusters 1, 2, and 3, poppy pixels (expected NDVI around 0.6–0.7) in clusters 1, 3, and 4, and miscellaneous pixels in clusters 0 and 4.

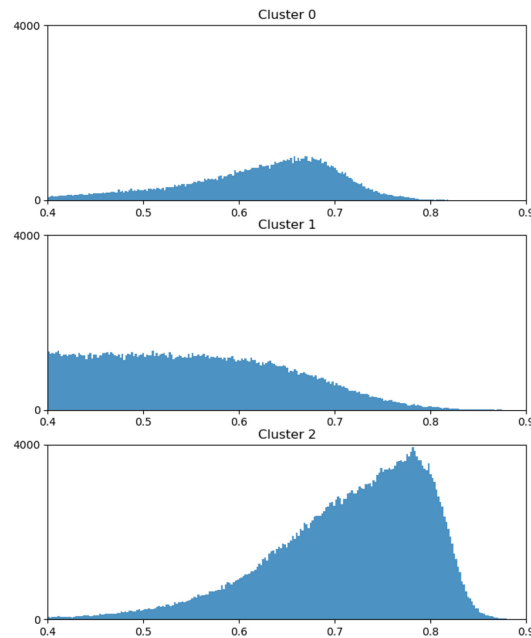


Fig. A.3. Results for GMM with three clusters, for 2019.

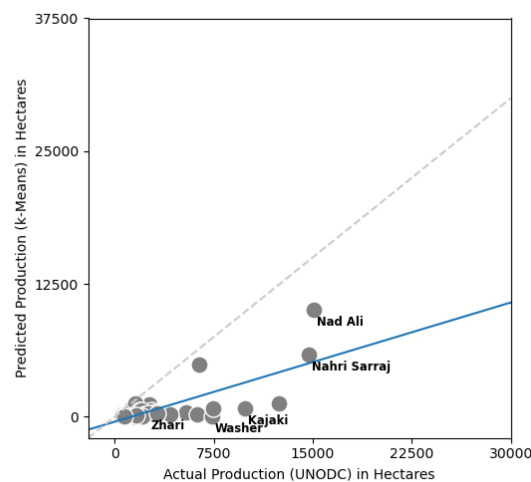


Fig. A.4. t-SNE plot shows the separation between the three clusters for pixels in the model training region in 2019.

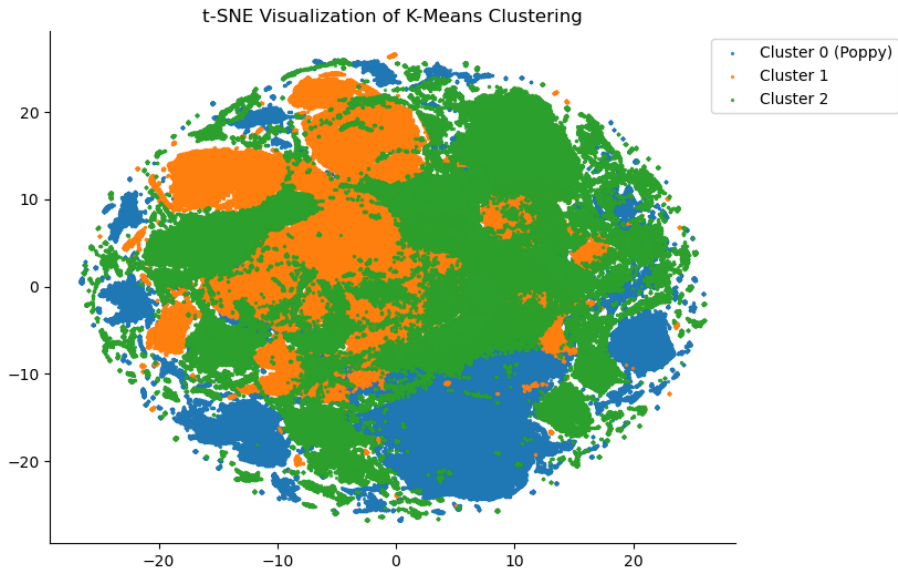


Fig. A.5. Distribution of NDVI values from pre-harvest pixels of the model training region, by fitted cluster number, in 2020 and 2021. We identify clusters 1 and 2, respectively, to be the clusters corresponding to poppy in 2020 and 2021.

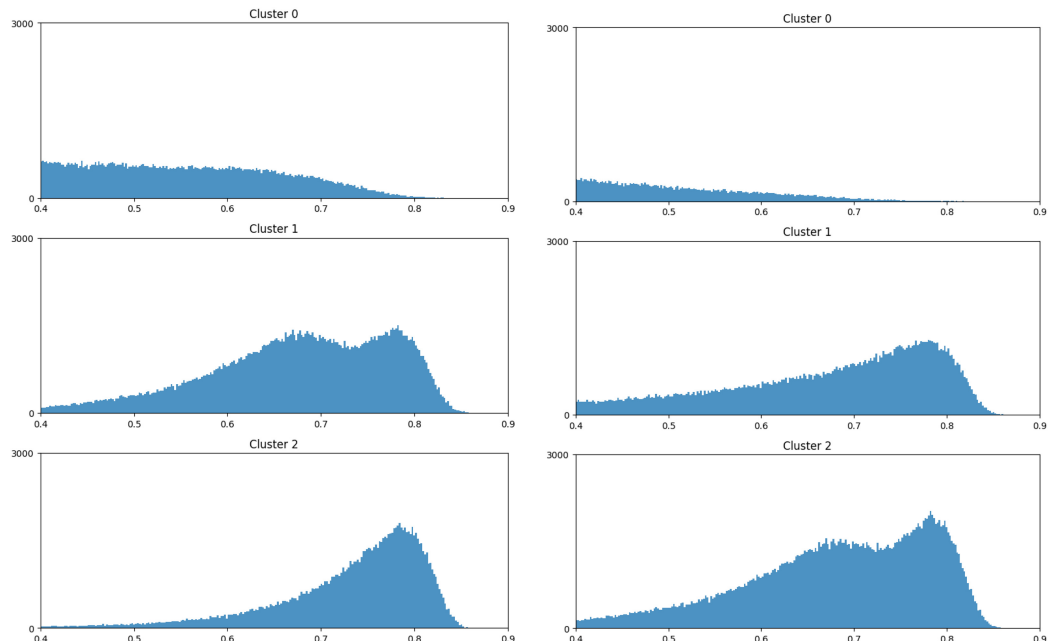


Fig. A.6. Distribution of geographic and climatic variables in agricultural grid cells that are classified as having no poppy cultivation in 2019, versus those that have any amount of poppy cultivation.

B APPENDIX B: REPRODUCIBILITY

Our analysis was carried out in a compute environment composed of two 12 core Intel Xeon Silver 4214R 2.4 G CPUs with 768 GB RAM. This is not a requirement but an artifact of our implementation. Note that somebody interested in running the study end-to-end might be required to adjust some of the parameters—including grid-cell resolution, number of CPU cores to be used and so on. – based on the specifications of the environment in which this code is run. Required parameters are fully described and documented.

All of the code used for this analysis is made publicly available at <https://github.com/arogyakoirala/poppy>. This contains roughly 1,700 lines of Python (Python 3.9.7) code that have been extensively documented for public dissemination. No non-standard packages are used, and all required packages and their versions are documented in a requirements.txt file.

Step-by-step instructions for scripts that execute the four stages required to generate the maps – data preparation, download, model fitting, and prediction—along with descriptions of required arguments have also been documented. All of the data inputs required for the analysis, with the exception of the Sentinel-2 imagery, are set up in the data preparation step. This includes ground truth cultivation statistics from UNODC, a district-level geopackaged shapefile for Afghanistan, geopackaged shapefiles for modelling regions within Zhari and Nad Ali, and the Copernicus Global Land Cover crop mask.

Sentinel-2 imagery from Google Earth Engine is downloaded separately using the download.sh script in the data download step, and image extraction and processing is carried out as described in Section 3.3. We reverse the order of operations in the implementation to allow parallelization of the imagery download (at the 50 km grid level), while preserving the same results. To be clear, in the implementation we first generate 50 km grid cells, and within each 50 km grid cell, acquire Sentinel-2 imagery for every qualifying 250 m tile, from Google Earth Engine.

With the downloaded and processed data, the model is fit and maps for all districts that we analyze are produced in the fitting and prediction stage (fit.py and predict.py). Rasters of cultivation maps are available as Google Earth Engine assets. For the socioeconomic analysis, poppy cultivation rasters were combined with other raster data sets on Google Earth Engine. Links to Earth Engine code are provided in the GitHub repository.

REFERENCES

- [1] John T. Abatzoglou, Solomon Z. Dobrowski, Sean A. Parks, and Katherine C. Hegewisch. 2018. TerraClimate, a high-resolution global dataset of monthly climate and climatic water balance from 1958–2015. *Scientific Data* 5, 1 (2018), 1–12.
- [2] James Richard Anderson. 1976. *A Land use and Land Cover Classification System for use with Remote Sensor Data*. Vol. 964. US Government Printing Office.
- [3] Rui Ba, Chen Chen, Jing Yuan, Weiguo Song, and Siuming Lo. 2019. SmokeNet: Satellite smoke scene detection using convolutional neural network with spatial and channel-wise attention. *Remote Sensing* 11, 14 (2019), 1702.
- [4] World Bank. 2020. World Bank Open Data. Retrieved from <https://data.worldbank.org/indicator/AG.LND.ARBL.ZS?locations=A>
- [5] Chahat Bansal, Hari Om Ahlawat, Mayank Jain, Om Prakash, Shivani A. Mehta, Deepanshu Singh, Harshavardhan-sushil Baheti, Suyash Singh, and Aaditeshwar Seth. 2021. IndiaSat: A Pixel-Level Dataset for Land-Cover Classification on Three Satellite Systems-Landsat-7, Landsat-8, and Sentinel-2. In *Proceedings of the ACM SIGCAS Conference on Computing and Sustainable Societies*. 147–155.
- [6] Linda A. Bartlett, Shairose Mawji, Sara Whitehead, Chadd Crouse, Suraya Dalil, Denisa Ionete, and Peter Salama. 2005. Where giving birth is a forecast of death: Maternal mortality in four districts of Afghanistan, 1999–2002. *The Lancet* 365, 9462 (2005), 864–870.
- [7] Allison L. Bennington. 2008. Application of multi-spectral remote sensing for crop discrimination in Afghanistan. (2008), 18–23.
- [8] Fatih Bicakli, Gordana Kaplan, and Abduldaem S. Alqasemi. 2022. Cannabis sativa L. spectral discrimination and classification using satellite imagery and machine learning. *Agriculture* 12, 6 (2022), 842.

- [9] Jelena Bjelica. 2020. New world drug report: Opium production in Afghanistan remained the same in 2019. *Afghanistan Analysts Network* 6, 25 (2020). Retrieved from <https://www.afghanistan-analysts.org/en/reports/economy-development-environment/new-world-drug-report-opium-production-in-afghanistan-remained-the-same-in-2019/>
- [10] Joshua Blumenstock. 2018. Don't Forget People in the use of Big Data for Development. *Nature* 561, 7722 (2018), 170–172.
- [11] Morgan Briggs. 2021. SatDash: An interactive dashboard for assessing land damage in Nigeria and Mali. In *Proceedings of the ACM SIGCAS Conference on Computing and Sustainable Societies*. 100–114.
- [12] Marcel Buchhorn, Myroslava Lesiv, Nandin-Erdene Tsendsazar, Martin Herold, Luc Bertels, and Bruno Smets. 2020. Copernicus global land cover layers—collection 2. *Remote Sensing* 12, 6 (2020), 1044.
- [13] Marshall Burke, Anne Driscoll, David B. Lobell, and Stefano Ermon. 2021. Using satellite imagery to understand and promote sustainable development. *Science* 371, 6535 (2021), eabe8628.
- [14] Roy Burstein, Nathaniel J. Henry, Michael L. Collison, Laurie B. Marczak, Amber Sligar, Stefanie Watson, Neal Marquez, Mahdieh Abbasalizad-Farhangi, Masoumeh Abbasi, Foad Abd-Allah, et al. 2019. Mapping 123 million neonatal, infant and child deaths between 2000 and 2017. *Nature* 574, 7778 (2019), 353–358.
- [15] Guanghua Chi, Han Fang, Sourav Chatterjee, and Joshua E. Blumenstock. 2022. Microestimates of wealth for all low- and middle-income countries. *Proceedings of the National Academy of Sciences* 119, 3 (2022), e2113658119.
- [16] S. Chuansiri, F. Blasco, M. F. Bellan, and L. Kergoat. 1997. A poppy survey using high resolution remote sensing data. *International Journal of Remote Sensing* 18, 2 (1997), 393–407.
- [17] Giacomo Falchetta, Shonali Pachauri, Simon Parkinson, and Edward Byers. 2019. A high-resolution gridded dataset to assess electrification in sub-Saharan Africa. *Scientific data* 6, 1 (2019), 110.
- [18] Saskia Foerster, Klaus Kaden, Michael Foerster, and Sibylle Itzerott. 2012. Crop type mapping using spectral-temporal profiles and phenological information. *Computers and Electronics in Agriculture* 89 (2012), 30–40.
- [19] Center for International Earth Science Information Network (CIESIN). 2020. *Food Insecurity Hotspots Data Set*. Technical Report. Socioeconomic Data and Applications Center.
- [20] Thomas Gibbons-Neff and Taimoor Shah. 2021. In hard times, afghan farmers are turning to opium for security. *The New York Times* 11, 21 (2021). Retrieved from <https://www.nytimes.com/2021/11/21/world/asia/afghanistan-crops-opium-taliban.html?searchResultPosition=23>
- [21] Anant Gulgulia, Aman Gupta, Akshay P. Sarashetti, Aaditya Sinha, and Aaditeshwar Seth. 2023. Tracking socio-economic development in rural india over two decades using satellite imagery. *ACM Journal on Computing and Sustainable Societies* 1, 2 (2023), 1–31.
- [22] Wes Harris. 2012. *Agricultural Review of Helmand Province, Afghanistan*. Technical Report. Agricultural Development for Afghanistan Pre-deployment Training. Retrieved from http://fresnostate.edu/jcast/ifa/documents/pdf/adapt_HELMAND.pdf
- [23] Alfredo Huete, Kamel Didan, Tomoaki Miura, E. Patricia Rodriguez, Xiang Gao, and Laerte G. Ferreira. 2002. Overview of the radiometric and biophysical performance of the MODIS vegetation indices. *Remote Sensing of Environment* 83, 1-2 (2002), 195–213.
- [24] Jordi Inglada, Marcela Arias, Benjamin Tardy, Olivier Hagolle, Silvia Valero, David Morin, Gérard Dedieu, Guadalupe Sepulcre, Sophie Bontemps, Pierre Defourny, et al. 2015. Assessment of an operational system for crop type map production using high temporal and spatial resolution satellite optical imagery. *Remote Sensing* 7, 9 (2015), 12356–12379.
- [25] Andy Jarvis, Hannes Isaak Reuter, Andrew Nelson, Edward Guevara, et al. 2008. Hole-filled SRTM for the globe Version 4. Available From the CGIAR-CSI SRTM 90m Database (<http://srtm.cgiar.org>) 15, 25–54 (2008), 5.
- [26] Neal Jean, Marshall Burke, Michael Xie, W. Matthew Davis, David B. Lobell, and Stefano Ermon. 2016. Combining satellite imagery and machine learning to predict poverty. *Science* 353, 6301 (2016), 790–794.
- [27] Shunping Ji, Chi Zhang, Anjian Xu, Yun Shi, and Yulin Duan. 2018. 3D convolutional neural networks for crop classification with multi-temporal remote sensing images. *Remote Sensing* 10, 1 (2018), 75.
- [28] Kun Jia, Bingfang Wu, Yichen Tian, Qiangzi Li, and Xin Du. 2011. Spectral discrimination of opium poppy using field spectrometry. *IEEE Transactions on Geoscience and Remote Sensing* 49, 9 (2011), 3414–3422.
- [29] Stefan Kienberger, Raphael Spiekermann, Dirk Tiede, Irmgard Zeiler, and Coen Bussink. 2017. Spatial risk assessment of opium poppy cultivation in Afghanistan: integrating environmental and socio-economic drivers. *International Journal of Digital Earth* 10, 7 (2017), 719–736.
- [30] Jo Thori Lind, Karl Ove Moene, and Fredrik Willumsen. 2014. Opium for the masses? Conflict-induced narcotics production in Afghanistan. *Review of Economics and Statistics* 96, 5 (2014), 949–966.
- [31] Xiangyu Liu, Yichen Tian, Chao Yuan, Feifei Zhang, and Guang Yang. 2018. Opium poppy detection using deep learning. *Remote Sensing* 10, 12 (2018), 1886.
- [32] Zifei Luo, Wenzhu Yang, Ruru Gou, and Yunfeng Yuan. 2023. TransAttention U-Net for semantic segmentation of poppy. *Electronics* 12, 3 (2023), 487.

- [33] David Mansfield. 2018. Turning deserts into flowers: Settlement and poppy cultivation in southwest Afghanistan. *Third World Quarterly* 39, 2 (2018), 331–349.
- [34] David Mansfield. 2019. On the frontiers of development: Illicit poppy and the transformation of the deserts of southwest Afghanistan. *Journal of Illicit Economies and Development* 1, 3 (2019), 330–345.
- [35] David Mansfield and Adam Pain. 2011. Evidence from the field: Understanding changing levels of opium poppy cultivation in Afghanistan. *The Politics of Narcotic Drugs: A Survey* (2011), 8–30.
- [36] Maureen Mayhew, Peter M. Hansen, David H. Peters, Anbrasi Edward, Lakhwinder P. Singh, Vikas Dwivedi, Ashraf Mashkoor, and Gilbert Burnham. 2008. Determinants of skilled birth attendant utilization in Afghanistan: A cross-sectional study. *American Journal of Public Health* 98, 10 (2008), 1849–1856.
- [37] M. Menenti, S. Azzali, W. Verhoeven, and R. Van Swol. 1993. Mapping agroecological zones and time lag in vegetation growth by means of Fourier analysis of time series of NDVI images. *Advances in Space Research* 13, 5 (1993), 233–237.
- [38] Jacob Metcalf and Kate Crawford. 2016. Where are human subjects in big data research? The emerging ethics divide. *Big Data & Society* 3, 1 (2016), 2053951716650211.
- [39] Local Burden of Disease Educational Attainment Collaborators. 2020. Mapping disparities in education across low- and middle-income countries. *Nature* 577, 7789 (2020), 235–238. DOI:<https://doi.org/10.1038/s41586-019-1872-1>
- [40] Darius Phiri and Justin Morgenroth. 2017. Developments in landsat land cover classification methods: A review. *Remote Sensing* 9, 9 (2017), 967.
- [41] James A. Piazza. 2012. The opium trade and patterns of terrorism in the provinces of Afghanistan: An empirical analysis. *Terrorism and Political Violence* 24, 2 (2012), 213–234.
- [42] Antonio J. Rivera, Maria D. Perez-Godoy, David Elizondo, Lipika Deka, and Maria J. del Jesus. 2022. Analysis of clustering methods for crop type mapping using satellite imagery. *Neurocomputing* 492 (2022), 91–106.
- [43] Robert A. Rohde and Zeke Hausfather. 2020. The berkeley earth land/ocean temperature record. *Earth System Science Data* 12, 4 (2020), 3469–3479.
- [44] Luke Sherman, Jonathan Proctor, Hannah Druckenmiller, Heriberto Tapia, and Solomon M. Hsiang. 2023. *Global High-Resolution Estimates of the United Nations Human Development Index Using Satellite Imagery and Machine-learning*. Technical Report. National Bureau of Economic Research.
- [45] Daniel M. Simms, Toby W. Waine, and John C. Taylor. 2017. Improved estimates of opium cultivation in Afghanistan using imagery-based stratification. *International Journal of Remote Sensing* 38, 13 (2017), 3785–3799.
- [46] Daniel M. Simms, Toby W. Waine, John C. Taylor, and Timothy R. Brewer. 2016. Image segmentation for improved consistency in image-interpretation of opium poppy. *International Journal of Remote Sensing* 37, 6 (2016), 1243–1256.
- [47] Daniel M. Simms, Toby W. Waine, John C. Taylor, and Graham R. Juniper. 2014. The application of time-series MODIS NDVI profiles for the acquisition of crop information across Afghanistan. *International Journal of Remote Sensing* 35, 16 (2014), 6234–6254.
- [48] Jeroen Smits and Iñaki Permanyer. 2019. The subnational human development database. *Scientific Data* 6, 1 (2019), 1–15.
- [49] John F. Sopko. 2018. *Counternarcotics: Lessons from the U.S. Experience in Afghanistan*. Technical Report. SPECIAL INSPECTOR GENERAL FOR AFGHANISTAN RECONSTRUCTION ARLINGTON VA.
- [50] Prashant K. Srivastava, Dawei Han, Miguel A. Rico-Ramirez, Michaela Bray, and Tanvir Islam. 2012. Selection of classification techniques for land use/land cover change investigation. *Advances in Space Research* 50, 9 (2012), 1250–1265.
- [51] Ralph Sundberg and Erik Melander. 2013. Introducing the UCDP georeferenced event dataset. *Journal of Peace Research* 50, 4 (2013), 523–532.
- [52] Andrew J. Tatem. 2017. WorldPop, open data for spatial demography. *Scientific Data* 4, 1 (2017), 1–4.
- [53] Varun Tiwari, Mir A. Matin, Faisal M. Qamer, Walter Lee Ellenburg, Birendra Bajracharya, Krishna Vadrevu, Begum Rabeya Rushi, and Waheedullah Yusafi. 2020. Wheat area mapping in Afghanistan based on optical and SAR time-series images in Google Earth Engine cloud environment. *Frontiers in Environmental Science* 8 (2020), 77.
- [54] United Nations Office on Drugs and Crime. 2016. *Afghanistan Opium Survey 2016*. Technical Report.
- [55] United Nations Office on Drugs and Crime. 2021. *Afghanistan Opium Survey 2019*. Technical Report.
- [56] United Nations Office on Drugs and Crime. 2021. *Drug Situation in Afghanistan 2021: Latest Findings and Emerging Threats*. Technical Report.
- [57] United Nations Office on Drugs and Crime. 2022. *Afghanistan Opium Survey 2021*. Technical Report.
- [58] United Nations Office on Drugs and Crime. 2023. *World Drug Report 2023*. Technical Report.
- [59] Laurens Van der Maaten and Geoffrey Hinton. 2008. Visualizing data using t-SNE. *Journal of Machine Learning Research* 9, 11 (2008), 2579–2605.
- [60] Jian-Jun Wang, Yun Zhang, and Coen Bussink. 2014. Unsupervised multiple endmember spectral mixture analysis-based detection of opium poppy fields from an EO-1 Hyperion image in Helmand, Afghanistan. *Science of the Total Environment* 476 (2014), 1–6.

- [61] Jian-Jun Wang, Guisheng Zhou, Yun Zhang, Coen Bussink, Jiahua Zhang, and Hao Ge. 2016. An unsupervised mixture-tuned matched filtering-based method for the remote sensing of opium poppy fields using EO-1 Hyperion data: An example from Helmand, Afghanistan. *Remote Sensing Letters* 7, 10 (2016), 945–954.
- [62] Sherrie Wang, George Azzari, and David B. Lobell. 2019. Crop type mapping without field-level labels: Random forest transfer and unsupervised clustering techniques. *Remote Sensing of Environment* 222 (2019), 303–317.
- [63] D. J. Weiss, A. Nelson, C. A. Vargas-Ruiz, K. Gligorić, S. Bavadekar, E. Gabrilovich, A. Bertoza-Villa, J. Rozier, H. S. Gibson, T Shekel, et al. 2020. Global maps of travel time to healthcare facilities. *Nature Medicine* 26, 12 (2020), 1835–1838.
- [64] D. J. Weiss, Andy Nelson, H. S. Gibson, W. Temperley, Stephen Peedell, Allie Lieber, Matt Hancher, Eduardo Poyart, Simão Belchior, Nancy Fullman, Bonnie Mappin, E. Cameron, U. Dalrymple, Jennifer Rozier, Tim Lucas, Rosalind E Howes, Lucy S Tusting, Su Yun Kangl, Donal Bisanzio, Katherine Battle, S. Bhatt, and P. W. Gething. 2018. A global map of travel time to cities to assess inequalities in accessibility in 2015. *Nature* 553, 7688 (2018), 333–336.
- [65] Evan Wigton-Jones. 2021. The unintended harms of infrastructure: Opium and road construction in Afghanistan. *Journal of Comparative Economics* 49, 2 (2021), 405–424.
- [66] Shiqi Yu, Sen Jia, and Chunyan Xu. 2017. Convolutional neural networks for hyperspectral image classification. *Neurocomputing* 219 (2017), 88–98.
- [67] Jun Zhou, Yichen Tian, Chao Yuan, Kai Yin, Guang Yang, and Meiping Wen. 2019. Improved uav opium poppy detection using an updated yolov3 model. *Sensors* 19, 22 (2019), 4851.

Received 30 June 2023; revised 20 November 2023; accepted 16 January 2024